JOURNAL OF MATERIALS SCIENCE 10 (1975) 2146–2155

Direct observation of liquid-phase sintering in the system iron-copper

LEONHARD FROSCHAUER, RICHARD M. FULRATH
Inorganic Materials Research Division, Lawrence Berkeley Laboratory, and Department of Materials Science and Engineering, College of Engineering, University of California, Berkeley, California, USA

The hot-stage of a scanning electron microscope has been used to observe liquid-phase sintering in the system iron–copper. The densification behaviour of compacts of Fe and Cu particles were determined. The influence of particle size of both components and the amount of liquid phase developed were investigated. In samples with about 20 vol % liquid phase, the densification kinetics as observed by direct observation shows that no rearrangement takes place. In samples with 40 vol % liquid phase and particle sizes of 10 to 20 μm, some rearrangement was observed.

1. Introduction

Liquid-phase sintering, i.e. sintering where a proportion of the material being sintered is in the liquid state, is a common processing technique for a variety of systems, including metal, cermets and ceramics. The sintered material usually consists of grains of one or more phases solid at the sintering temperature intermixed with phase that is liquid at sintering temperature.

It is very important to understand the parameters that control the densification behaviour and the resulting microstructure (grain size and shape, pore size and shape, phase distribution, etc) because of their effect on the physical and chemical properties of the final product. The development of a theory to describe liquid phase sintering is difficult because:

(a) the existence of at least three phases at sintering temperature (solid, liquid, vapour) increases the number of parameters (especially boundary energies between phases, solubilities, quantities, liquid viscosities);

(b) changing boundary energies and solubilities can change the microstructure during the cooling of the system to room temperature where the microstructure normally is observed;

(c) the often very fast shrinkage after the first appearance of the liquid phase makes it extremely difficult to stop the process in different states of morphology development.

For these reasons, most research work has followed the procedure of:

(a) determination of sintering behaviour (densification, microstructure development) and qualitatively explain the results, using known properties of the system;

(b) model calculations for possible densification processes and comparison of these calculations with the measured densification kinetics.

The availability of a hot stage for the scanning electron microscope (SEM) allows a new approach to the problem. Direct observation of the sintering has been tried before by hot-stage microscopy [1, 2] but the low depth of field makes this technique difficult. The hot stage of the SEM provides a means for continuous monitoring and filming of the microstructure development during the sintering process with a reasonable depth of field at high magnification.

2. General background

Sintering studies have been performed for many materials, a review article by Eremenko *et al.* [3] gives detailed description of the results. The main properties of the components and the system that influence the sintering behaviour have been listed in Table I.

Table II gives the proposed sintering mechanisms and the corresponding kinetics that result from model calculations. A description of

TABLE I Main influences on liquid-phase sintering

Property	Influence
Property of the solid phase	
Particle size and shape	Mobility of the particles for rearrangement. Necessary diffusion for solution-precipitation.
Properties of the liquid-forming phase	
(a) Particle size and shape (?)	Pore size after melting for large liquid-forming particles.
(b) Viscosity	Viscosity of whole sample (rearrangement). Penetration into crevices between solid particles.
Common properties	
(a) Wetting behaviour (characterized by contact and dihedral angle)	Capillary forces for densification. Penetration into gaps between solid particles (rearrangement and solution-precipitation).
(b) Solubilities	
Liquid in solid	Amount of liquid phase changes during sintering.
Solid in liquid	Solution of necks. Solution-precipitation process.
(c) Quantities	Viscosity of sample (rearrangement). Porosity after rearrangement.
(d) Green density	Ability of solid particles to rearrange (interlocking).
(e) Relative melting points	Neck-growth of solid phase during heating. Change in apparent particle size.

TABLE II Proposed sintering mechanisms and kinetics

Reference	Process	Kinetics	Assumptions
Price *et al.* [4]	"Heavy alloy mechanism" "Ostwald ripening"		
Kingery [5]	Rearrangement Solution-precipitation	$\Delta L/L_0 \sim t^{1+y}$ $y \ll 1$ (a) $\Delta L/L_0 \sim r^{-4/3} t^{1/3}$ spheres $\Delta L/L_0 \sim t^{1/5}$ prisms (b) $\sim r^{-1} t^{1/2}$ spheres $\sim t^{1/3}$ prisms (a) diffusion-controlled (b) solution-controlled	Complete wetting zero dihedral angle for solution-precipitation-process solubility of solid in liquid
Cech [6]	Viscous flow	$\Delta L/L_0 = K_1(\log t - \log t_0) - K_2(t^4 - t_K^4) + K_3 t^{1/3}$	Entrapped gas in pores Pores close at t_K Term 3 for gas diffusion
Gessinger *et al.* [7]	Solution-precipitation	Time exponent 0.3125 to 0.333 changing with liquid volume, dihedral angle and shrinkage	Sphere model

TABLE III Important properties of three systems for LPS

System	$\frac{T_m \text{ (liquid)}}{T_m \text{ (solid)}}$	Contact angle		Dihedral angle	Solubility solid in liquid
Fe–Cu	0.79	0° (H_2)	[8]	27°	5%
W–Cu	0.37	30° 1150° C (H_2) 0° 1350° C	[15]	–	none
WC–Co	0.60	0° (vacuum)	[14]	probably 0° (see Discussion in [8])	40%

these mechanisms can be found in review articles (e.g. [8]) or in the original literature.

For the initial studies using the SEM hot stage, it was intended to use systems with a model character that have been investigated previously. Three systems, Fe–Cu, WC–Co, and W–Cu were chosen; the main properties for (sintering) of these systems are listed in Table III. This first part deals with the results for Fe–Cu. The system Fe–Cu is of special interest both from a theoretical and practical point of view.

Ramakrishnan [9], Cannon [10] and Kingery [11] find during the first minutes after liquid development a time-proportional shrinkage. Kinergy used this system to prove the existence of a rearrangement process in the early stages of densification, for which his theory predicted

$$\Delta L/L_0 \sim t^{1+y} \quad (y \ll 1).$$

This densification mechanism seems to be widely accepted for Fe–Cu [8], in spite of the fact that the properties of the system do not meet the requirements of Kinergy's model. He assumes complete wetting of the two phases with a dihedral angle of 0°, so that the liquid penetrates into the gaps between iron particles. The dihedral angle in this system, however, has been measured as 27° (Table III). Following this fast densification, a second stage is proposed in which a dependence

$$\Delta L/L_0 \sim t^{1/3}$$

seems to describe the results. Again referring to Kingery's models, a solution-precipitation process is assumed. But there again the model uses the assumption of zero dihedral angle that leads to no particle–particle contacts. Microstructure observations showed strong neck growth in very short times and a very fast particle growth. Whalen and Humenik [12] report that within 20 min the average particle size changes from 10 μm to 30 μm.

3. Experimental procedure

3.1. Sample preparation

The starting powders were spherical iron and copper particles that were sieved into different size fractions. The size fractions were 10 to 20 μm and $< 37\,\mu$m for iron, 10 to 20 μm and $< 44\,\mu$m for copper. Mixtures of the powders were prepared with 10 to 50 vol% copper and mixed in alcohol for 24 h.

Samples 3/16 in. diameter and approximately 1/8 in. thick were cold-pressed with about 200 MN m^{-2}, this resulted in green densities of about 70% theoretical density. To remove oxide films from the particle surfaces, all samples were prefired for 1 h at 450° C in helium–4% hydrogen.

3.2. Sintering

The sintering was carried out in vacuum in the hot stage of a scanning microscope. An older design of the hot stage has been described previously [13]. Minor modifications have resulted in a stage that can operate at temperatures over 1700° C. The sample rests in a molybdenum cup inside the heating element. Temperature was determined by a thermocouple welded to the bottom of a flat stand supporting the sample cup. For shrinkage measurements, the SEM was operated at low magnifications of about × 100; alumina spheres on the sample surface served as markers to determine the shrinkage. Fig. 1 shows a sample surface during sintering with marker spheres.

The screen of a TV monitor was recorded on film by a camera that allowed continuous framing with speeds of 1 to 0.1 frames/second. The distances between the markers are measured from the film. For the observation of microstructure, the SEM can be operated at magnifications up to × 5000.

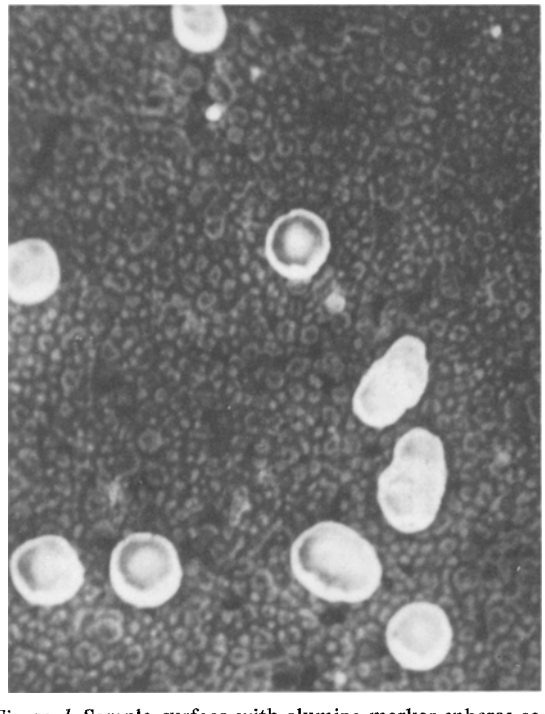

Figure 1 Sample surface with alumina marker spheres as photographed from the SEM TV monitor screen.

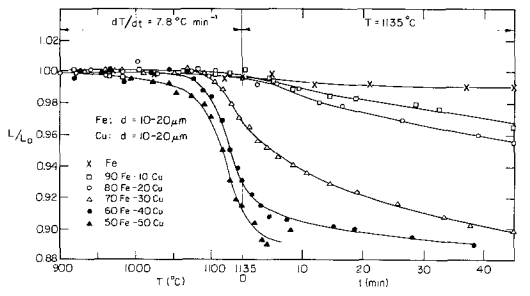

Figure 2.

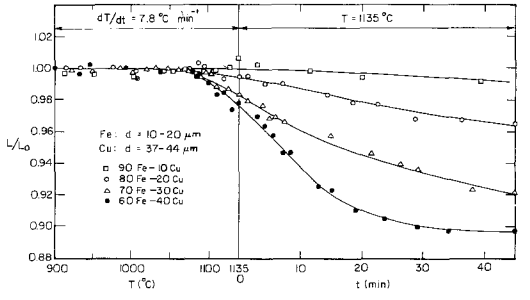

Figure 3.

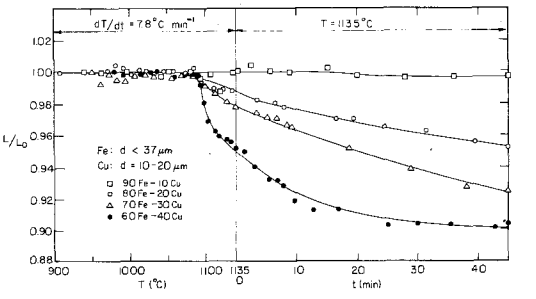

Figure 4.

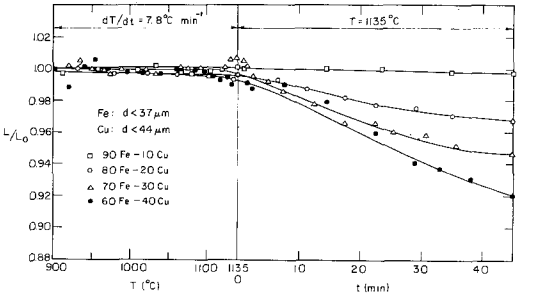

Figure 5.

Figures 2 to 5 Densification curves for iron–copper with different combinations of particle sizes of the two components and volume fractions of the components.

For all samples, the same heating cycle has been used. The material was heated to 900° C in 4 min, held isothermally for 5 min, and then was then heated at 7.8° C min^{-1} to 1135° C. The samples were held for 45 min at this temperature.

4. Results and discussion

4.1. Shrinkage

To find the influence of different parameters (content of liquid phase, particle size of both components), a series of experiments were performed. Figs. 2 to 5 show densification results for samples with different combinations of particle sizes.

In all cases the densification rate increases with increasing liquid content. This is in accordance with all proposed mechanisms, because rearrangement (due to fewer contact points between Fe–Fe particles), diffusion, and solution-controlled processes are enhanced by increasing the liquid phase content. (The very few exceptions from this behaviour are in systems with a high solubility of the liquid in the solid phase.)

The increase in densification with decreasing solid-phase particle size (Fig. 6) is also expected by the models. Smaller particles (of the same shape) have higher mobilities (for rearrangement) and need less material transport for solution-precipitation.

The influence of the size of the liquid forming

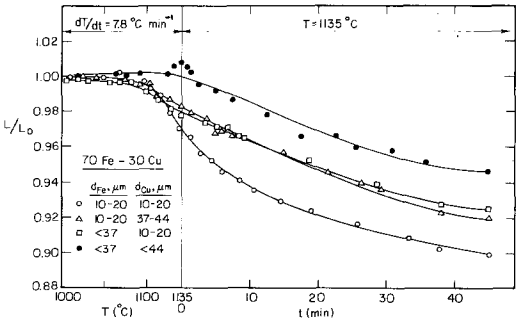

Figure 6 Densification of 70 Fe–30 Cu as a function of component particle sizes.

particles (Fig. 6) has not been reported previously. This effect can be explained as follows. After melting, the liquid phase is distributed in a continuous network of iron particles. In equilibrium, the small pores formed by the network will be filled with liquid phase and the large pores will be open, because the capillary forces increase with decreasing pore radius. For large liquid forming particles, their size determines the largest pore size, the large pores in the compact are the spaces previously held by Cu particles.

This can be seen in micrographs. Fig. 7 shows polished sections of different samples after sintering for 45 min. Even after this long time, the pores are roughly of the size of the original Cu particles. Fig. 8 shows samples of 80 Fe–20 Cu (both 10 to

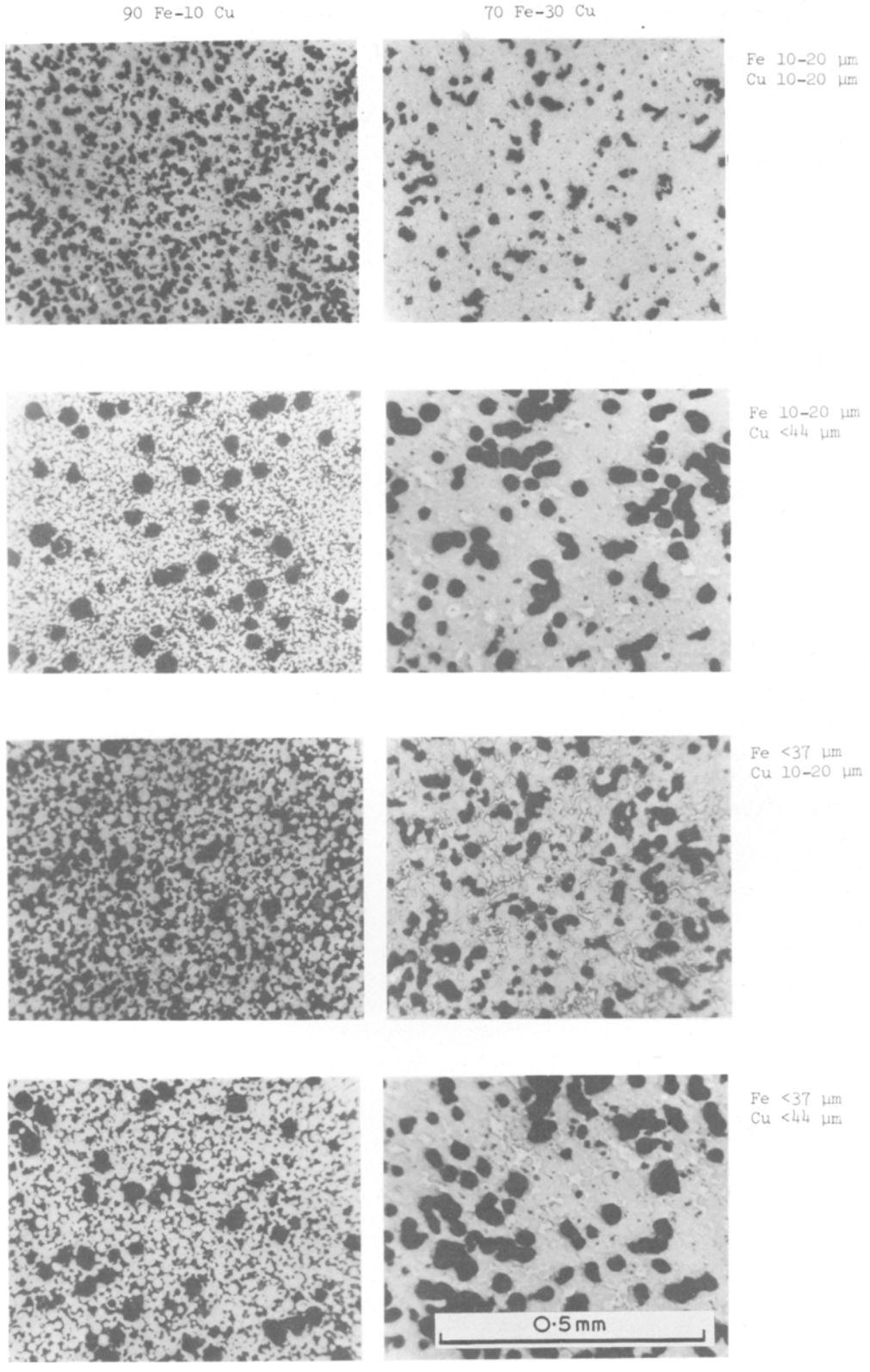

Figure 7 Microstructure developed after sintering for 45 min at 1135° C as a function of the particle sizes and the amount of liquid phase.

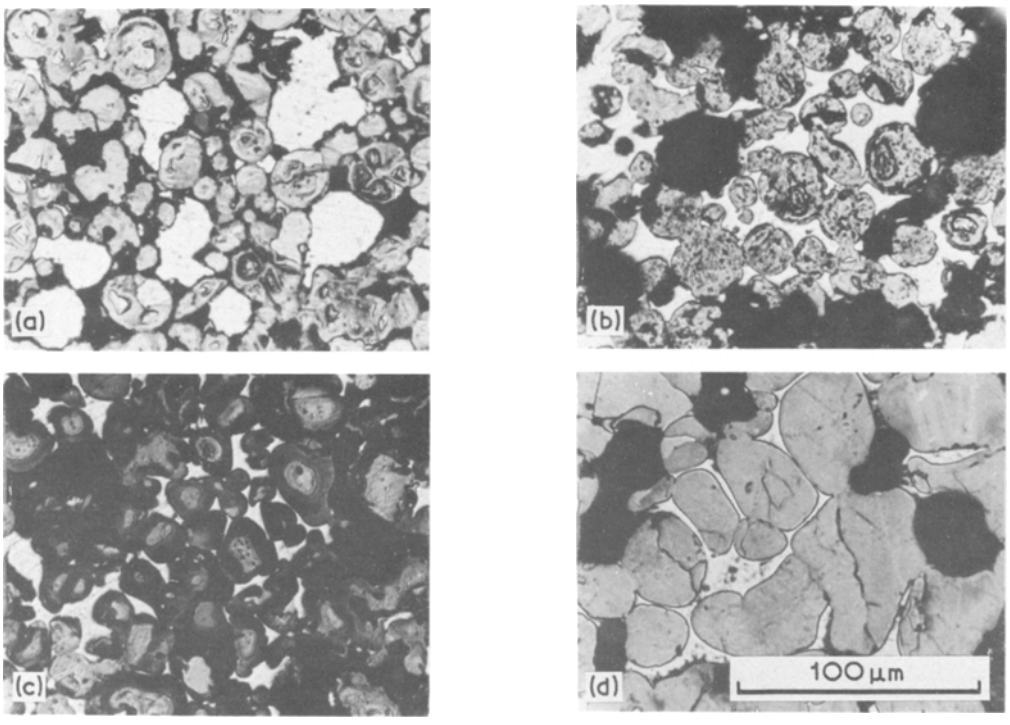

Figure 8 Microstructures of samples 80 Fe–20 Cu (10 to 20 μm) in different states: (a) before melting; (b) immediately after melting; (c) 5 min after melting; (d) 45 min after melting.

20 μm) in different states of the process. Between (a) and (b) of Fig. 8 the copper melted, the small pores in (a) have filled with Cu and large pores have appeared; their size corresponds to the Cu-particle size. After 45 min sintering (Fig. 8d) the large pores are still present. Large particle growth has occurred during this time at temperature.

To compare with these results with previous investigations, the results have been plotted on a log–log scale (Fig. 9). (As time zero, the time on reaching 1100° C was chosen.)

From these plots, two essential conclusions can be drawn: (1) the results are in general agreement with previous data; (2) results that show an abrupt change of slope from approximately 1 to $\frac{1}{3}$ are not observed. It seems rather reasonable to assume a continuing change in slope

4.2. Densification mechanism

Comparing the densification kinetics as shown in

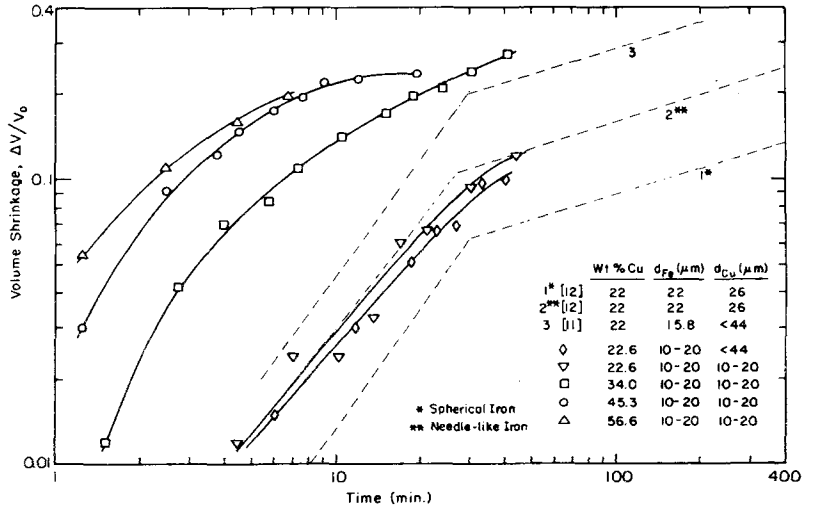

Figure 9 Volume shrinkage as a function of time for different samples (including literature results).

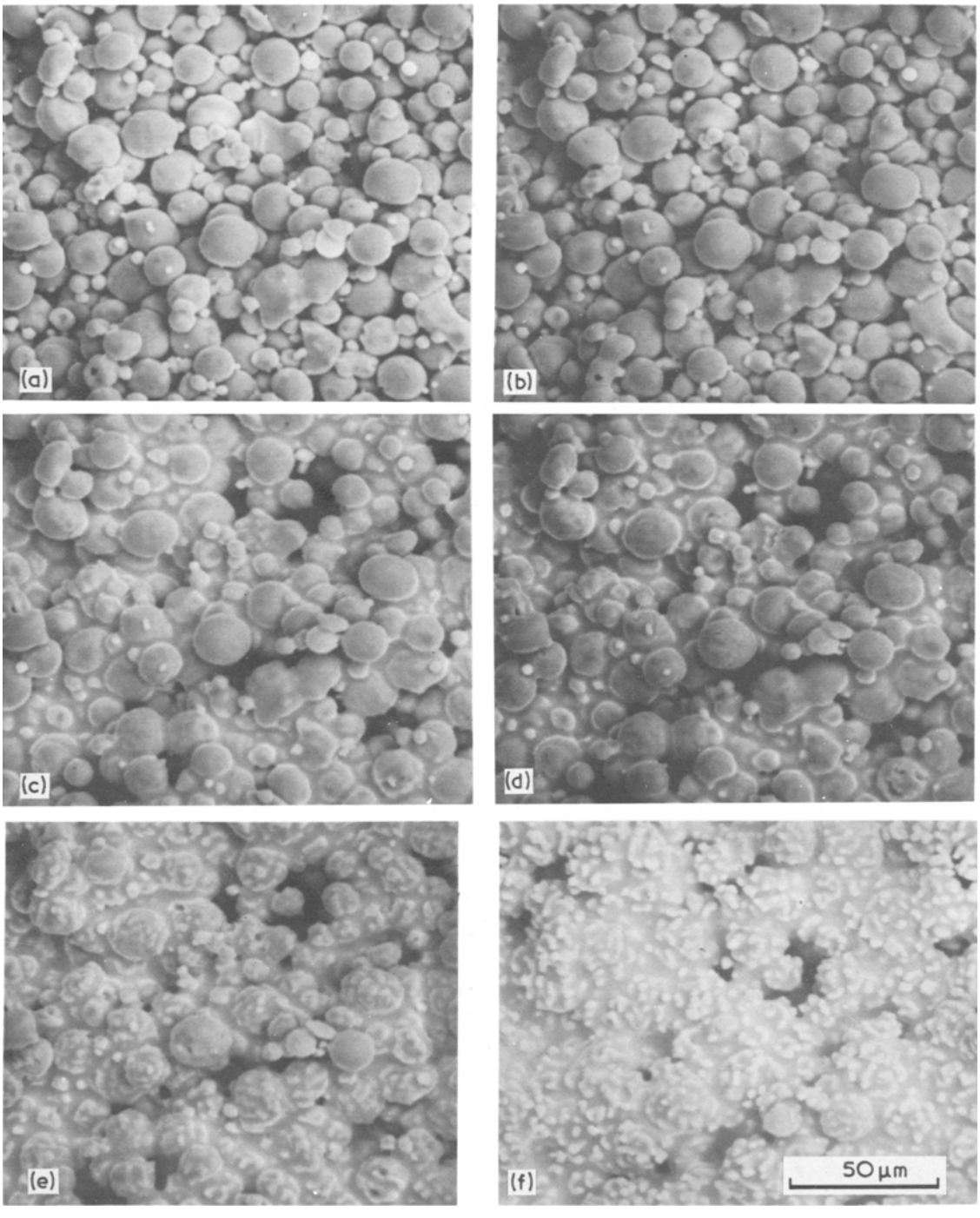

Figure 10 SEM hot stage pictures of a sample 80 Fe–20 Cu (both 10 to 20 µm) in stages of the heating and sintering process. (a) $t = 9.8$ min, $T = 830°$ C; (b) $t = 36.0$ min, $T = 1030°$ C; (c) $t = 42.5$ min, $T = 1090°$ C; (d) $t = 45.8$ min, $T = 1125°$ C; (e) $t = 55.5$ min, $T = 1135°$ C; (f) $t = 85.0$ min, $T = 1135°$ C.

Fig. 9 with the different models, it must be concluded that the first part of the densification is a rearrangement process, followed by a slower mechanism. For 80 Fe–20 Cu during the first 40 min, the densification follows rearrangement kinetics.

This could not be verified in direct observation. Figs. 10 to 12 show SEM pictures of samples with 20 and 40 vol % Cu during the sintering process. In the samples with 20% Cu, no indication of a

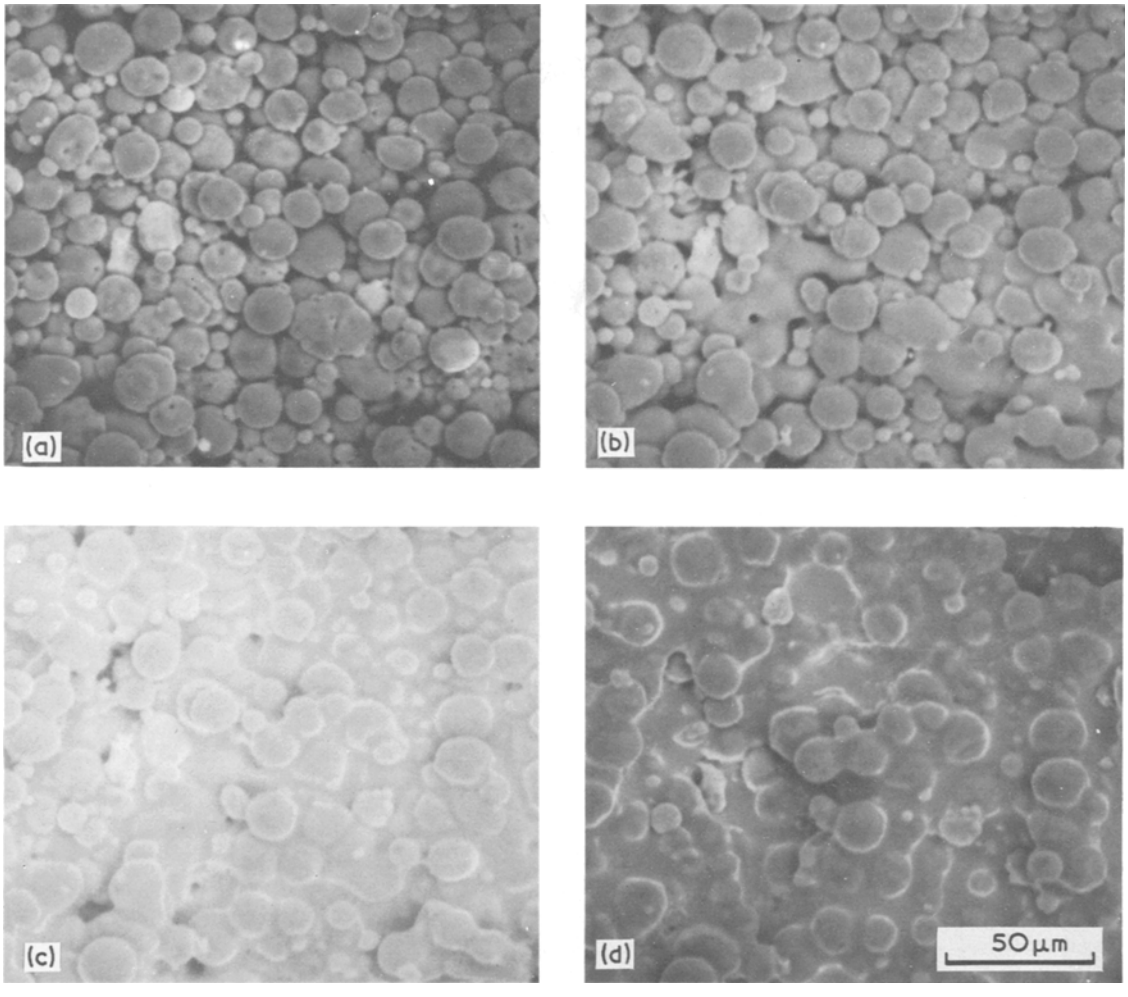

Figure 11 As Fig. 10 for a sample of 80 Fe–20 Cu (Fe < 37 µm, Cu < 44 µm). (a) $t = 6.5$ min, $T = 900°$ C; (b) $t = 35.2$ min, $T = 1080°$ C; (c) $t = 36.0$ min, $T = 1090°$ C; (d) $t = 37.8$ min, $T = 1105°$ C; (e) $t = 46.6$ min, $T = 1135°$ C.

change in the relative positions of the iron spheres can be found; in samples with 40% Cu (particle size 10 to 20 µm) some relative movement takes place (Fig. 12). This is more easily seen by viewing a continuous film.

Another result that strongly contradicts a rearrangement process is the neck growth during the heating of the samples to the melting temperature (Fig. 8a). After melting the liquid phase does not penetrate into these necks. This behaviour is predicted theoretically for a system with a dihedral angle of nearly 30° and can be confirmed in micrographs (Fig. 8b, c). For higher amounts of liquid phase, the number of solid neighbours and thus the probability for formation of a rigid skeleton decreases.

The hot-stage observations and the micrographs seem to prove that the densification in this system (liquid content 20%) is completely by a diffusion process. No rearrangement can be found. The

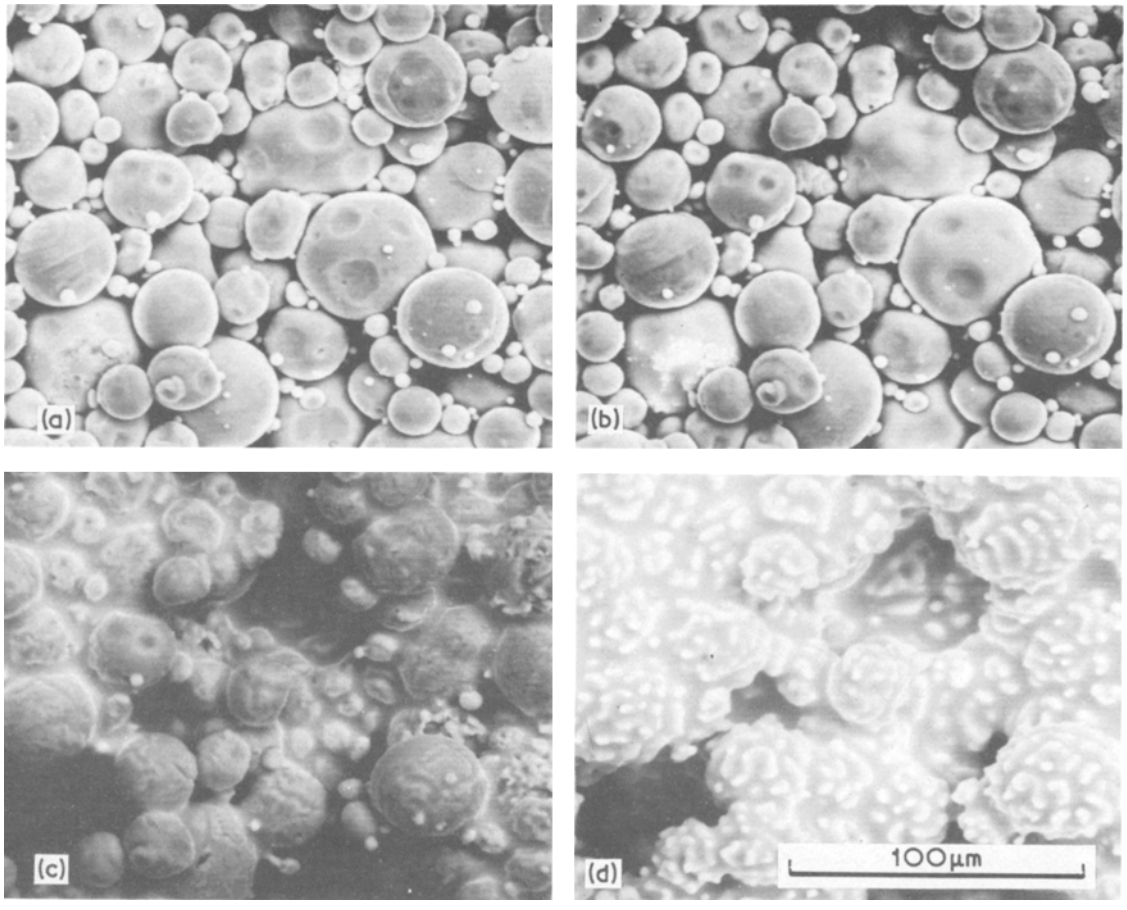

Figure 12 As Fig. 10 for a sample 60 Fe–40 Cu (both 10 to 20 μm). (a) $t = 0$ min, T = room temperature; (b) $t = 23.0$ min, $T = 970°$ C, (c) $t = 42.7$ min, $T = 1135°$ C; (d) $t = 72$ min, $T = 1135°$ C.

rapid particle growth and change of particle shape relative to the shape of the neighbours (see Fig. 8d) are hints that a solution-precipitation process dominates. The change in particle shape to give a close packing makes a process similar to that proposed by Kingery [5] probable. He assumed that near contact points the chemical potential and thus the solubility are increased due to stresses originating from the capillary forces.

This result suggests that it is not possible to define the densification mechanism in a non-complete wetting system by comparing the sintering kinetics with the results of existing model calculations. The main reason for the different behaviour is that in calculations for non-complete wetting systems, a regular array of solid spheres with uniform porosity is assumed. In real systems there is always a distribution of pore sizes and thus a distribution of the liquid phase where small pores (that would result in a large capillary pressure) are closed and large pores are open. A better fit to model calculations can be expected where the liquid-forming phase has a very small particle size compared to the solid phase.

5. Conclusions

Direct observation of the sintering processes in the hot stage of a scanning electron microscope can give important information not available in conventional techniques. At low magnifications the densification can be determined even for very fast shrinking samples. At high magnifications the microstructure can be observed continually as sintering progresses.

The determination of liquid-phase sintering in the system Fe–Cu showed that the densification rate is in general agreement with previous results, but the continuous determination of shrinkage proved that the densification is not, as previously assumed, a process with two distinct stages and an abrupt change in the time-dependence but rather a smooth transition with continuously changing

slope.

The direct observation of microstructure development showed that in this system for low amounts of liquid phase, no rearrangement in the early stages of densification can be found. This would be expected from data on neck and particle-growth and the wetting behaviour of Fe–Cu. It contradicts the densification kinetics assumed by comparing experiments with model calculations. New calculations for non-complete wetting systems regarding the actual pore-size and distribution seem necessary for further model calculations.

Acknowledgements

We thank Professor Joseph A. Pask for reviewing the manuscript and for many valuable comments. The work was supported by the United States Atomic Energy Commission through the Inorganic Materials Research Division of the Lawrence Berkeley Laboratory and by the Deutsche Forschungsgemeinschaft.

References

1. E. M. DAVER and W. F. ULLRICH, in "Perspectives of Powder Metallurgy", edited by J. S. Hirschhorn and K. H. Roll, (Plenum, New York, 1970) pp. 189–200.
2. N. DAUTZENBERG, *Arch. Eisenhüttenw.* **41** (1970) 1005.
3. V. N. EREMENKO, Yu. V. NAIDICH and I. A. LAVRINENKO, Special Report "Liquid Phase Sintering" translated from Russian (Consultants Bureau, New York, 1970).
4. T. PRICE, C. SMITHELLS and S. WILLIAMS, *J. Inst. Met.* **62** (1938) 239.
5. W. D. KINGERY, *J. Appl. Phys.* **30** (1959) 301.
6. B. CECH, *Sov. Powder Met.* **2** (1963) 86.
7. G. H. GESSINGER, H. F. FISCHMEISTER and H. L. LUKAS, *Acta Met.* **21** (1973) 715.
8. T. J. WHALEN and M. HUMENIK, in "Sintering and Related Phenomena", edited by G. Kuczynski, N. A. Hooton and C. F. Gibbon (Gordon and Breach, New York, 1967) pp. 715–46.
9. P. RAMAKRISHNAN and R. LAKSHMINARASIMHAN, *Int. J. Powder Met.* **3** (1967) 63.
10. H. S. CANNON and F. V. LENEL, "Plansee-Seminar Pulvermetallurgie" (Metallwerk Plansee AG., Reutte, Austria, 1953) pp. 106–21.
11. W. D. KINGERY and M. D. NARASHIMHAN, *J. Appl. Phys.* **30** (1959) 307.
12. T. J. WHALEN and M. HUMENIK, *Prog. Powder Met.* **18** (1962) 85.
13. R. M. FULRATH, Scanning Electron Microscopy to 1600° C in "Scanning Electron Microscopy 1972" (Part I), edited by O. Jahan and I. Corvin (IIT Research Institute, 1972) pp. 17–24.
14. L. RAMQUIST, *Int. J. Powder Met.* **1** (4) (1965) 2.
15. YU, V. NAIDICH, I. A. LAVRINENKO and V. N. EREMENKO, *ibid* **1** (4) (1965) 41.

Received 29 August 1974 and accepted 9 April 1975.